CH-89-5-2

Natural Convection in Sealed Glazing Units: A Review

J.L. Wright, P.Eng.
ASHRAE Student Member

H.F. Sullivan, Ph.D., P.Eng.
ASHRAE Member

ABSTRACT

In cold climates the augmented edge-glass heat transfer at the bottom of a glazing system creates a special problem. This is where condensed water and/or frost most readily occur. Two mechanisms determining the rate of edge-glass heat transfer, namely, edge-seal conduction and fill gas convection, are discussed. Current methods for estimating average edge-glass heat loss rates are reviewed. No reliable methods have been established for calculating the minimum temperature near the bottom of the indoor glazing. Heat transfer by natural convection of a gas in a vertical slot is a highly complex process about which there exists an abundance of technical information. The literature reviewed describes laminar flow regimes, mechanisms of heat transfer, local heat transfer, hydrodynamic stability, and conditions governing the onset of turbulence. These findings are discussed as they pertain to total and local heat transfer rates in glazing systems.

INTRODUCTION

Background

Conventional windows provide only a minimum level of thermal resistance and can create thermal comfort problems, very low allowable humidity levels, and damaging accumulations of condensed water and frost. These shortcomings strengthen the desire for windows with high thermal resistance—particularly in countries with cold climates.

Emerging technology is creating many opportunities for innovative glazing system design. Evidence of this progress exists in the wide variety of components being marketed and/or researched. Examples of new and technically advanced components include spectrally selective low-emissivity (low-e) coatings, solar control coatings, infrared (IR) transparent glazings, anti-reflective surface treatments, low-conductivity fill gases, silica aerogels, holographic glazings, optical switching glazings, polarized glazings, and evacuated enclosures. The energy-saving performance of windows incorporating some of these advanced features can be impressive.

Most windows manufactured today contain a glazing system that is packaged in the form of a sealed glazing unit (SGU). The SGU typically consists of two panes of glass that are separated from each other by an edge-spacer. This spacer seals off the cavity between the glazings—thereby reducing the number of surfaces to be cleaned and creating an insulating cavity suitable for nondurable, low-e coatings and/or substitute fill gases. In contrast to the glazing system, few options are commercially available to increase the thermal resistance of the SGU edge-seal. Design improvements have dealt mainly with the requirements of the edge-seal to exclude moisture, provide a desiccant for the sealed space, and retain the structural integrity of the SGU. Hence, the thermal bridge created by the edge-seal results in a band at the perimeter of the SGU where the temperature of a glazing can vary significantly as a function of distance from the edge of the glazing. This is an area of increased thermal stress in the glass (1), high energy loss, and the site of condensation during cold weather.

During cold weather, the convective flow of fill gas within the sealed space of an SGU is such that it contributes to the condensation problem at the bottom edge of the indoor glazing. Fill gas within the SGU sealed space flows upward near the indoor glazing and downward near the outdoor glazing. The descending gas becomes progressively colder. At the bottom of the cavity this cold fill gas turns and comes in direct contact with the bottom of the indoor glazing, where it starts its ascent. Thus, the glass near the bottom edge of the indoor glazing is cooled by the coldest fill gas in the interpane gap. A similar situation occurs at the top of the cavity where the fill gas heats the top of the outdoor glazing. Experimental results support the hypothesis that fill gas motion contributes to the bottom-edge condensation problem. Heat flux measurements using a guarded heater plate apparatus (2) have consistently shown that the heat flux to the bottom of the warm side glazing is higher than the heat flux to the top of the same glazing. Clearly, any model attempting to quantify local heat transfer rates in these regions or intended to determine the temperature distribution across the face of the glazing must account for both the edge-seal heat loss and the nature of the fill gas flow.

It is common for heat transfer through windows to be quantified by treating the frame and glazing areas independently. Recently SGU analysis methods have followed a similar course. The SGU can be divided into two areas. The "center-glass" area is the section of the glazing system that is sufficiently remote from the edge that the heat

John L. Wright, Research Engineer, and **H.F. Sullivan**, Professor, Department of Mechanical Engineering, University of Waterloo, Waterloo, Ontario, Canada.

transfer can be characterized as being independent of edge effects. Center-glass heat transfer is generally simulated as a one-dimensional phenomenon. The perimeter of the glazing system where the heat transfer is two-dimensional or three-dimensional and depends upon edge effects (such as the edge-seal conduction or the turning motion of the fill gas) is customarily called the "edge-glass" section.

Calculation and measurement techniques used prior to 1947 to estimate the thermal resistance of windows were reviewed in detail by Parmalee (3). Parmalee described the guarded hot box, calibrated hot box, and hot plate measurement techniques. He presented a large compilation of data and noted that a "considerable range" in measured U-value existed for "approximately similar windows." A calculation procedure was developed but was hindered by a lack of knowledge about either natural convection and/or forced convection at the exposed window surfaces or natural convection in the window cavity. Edge effects were neglected.

McCabe and Goss (4) have written an up-to-date review concerning hot-box test methods and calculation procedures. This document provides a discussion of the U.S. test standards (ASTM C296, ASTM C976, and AAMA 1503.6) plus copies of the Norwegian standard (NBI-138), the Swedish standard (SS81 81 29), the Belgian standard (NBN B62-002), and a working draft of the ASTM standard being developed (C16:30). A new Belgian standard for calculating thermal transmission coefficients (U-values) for windows is being developed. This work includes the effect of edge-glass heat transfer and is being prepared in support of the draft ISO standard that, as recently as May 1986 (5) did not account for heat loss through edge-seals. Many details of the draft ISO standard, including edge-glass heat loss calculation procedures, are presented by Curcija et al. (6).

Center-Glass Heat Transfer

The source that is most widely referenced for center-glass U-values is Table 13 in the fenestration chapter of the *ASHRAE Fundamentals*. This chapter also provides a procedure for hand calculation of center-glass U-values. Table 13 is currently being revised in order to include a wider variety of glazing system designs and to treat the center-glass, edge-glass, and frame heat transfer rates as separate quantities.

In light of the increasingly complex nature of glazing system design, as well as the fundamental differences in IR properties of some of the plastic films now available, it has become apparent that conventional calculation methods are no longer adequate. In order to fill this void and to support the effort at the National Research Council of Canada, a glazing system computer simulation program called VISION was written (7-11). VISION is a two-band (solar and thermal wavelengths) thermal analysis program. The thermal analysis algorithm used in VISION is based on the method presented in references 12, 13, and 14. VISION has been used as the basis for a variety of studies including the development of a simplified seasonal thermal performance calculation method (15-17). Several capabilities of VISION provide improvements over previous methods. These include the ability to model multiple glazings, sloped glazings, and substitute fill gases. The most significant improvement is the ability to model fully or partially IR-transparent glazings. Interpane convective heat transfer is handled using the correlations of ElSherbiny et al. (18). Another computer program that has many features in common with VISION has been produced in the United States. This program, called WINDOW, is based on the work of Rubin (19) and also incorporates the convection correlations found in reference 18.

Many laboratories around the world are capable of window U-value measurement. The majority of these facilities use the calibrated hot-box or guarded hot-box test method. Controversy exists regarding methods that are appropriate for producing prescribed indoor and outdoor (natural and forced) convective film coefficients during hot-box testing (3, 20) and heat transfer rates over specific portions of a glazing/frame assembly are difficult to isolate. Some researchers study heat transfer with windows expos-

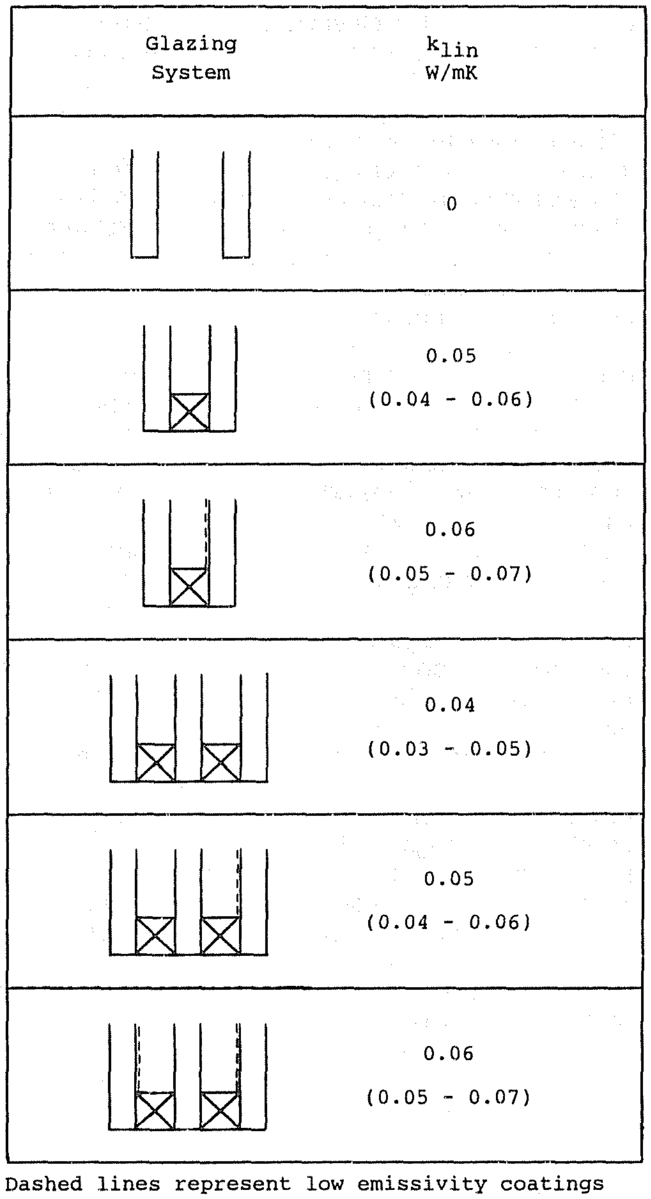

Figure 1 *Linear k-values used to estimate edge-seal heat loss (from Frank and Muhlebach 1987)*

ed to the outdoor environment (e.g., 21-24). Difficulties arising from this arrangement include the necessity to account for local wind speed and the radiative exchange between the window and the clear portion of the sky as well as the variability of the outdoor surroundings.

Edge-Glass Heat Transfer

Two calculation methods for estimating edge-glass heat transfer have very recently been devised. One method has resulted from a joint effort by researchers in Switzerland, Belgium, and France as part of the Windows and Fenestration Task of the International Energy Agency (IEA) Annex XII (Energy Conservation in Buildings and Community Systems Programme). IEA workers have proposed a set of edge-seal conductances or "linear k-values" (25) based on measurements and finite-difference calculations. The recommended linear k-values are shown in Figure 1. These k-values are multiplied by the length of the edge-seal in order to estimate the increase in heat loss caused by the seal. In other words, the center-glass conductance is applied over the entire glazed area and additional heat loss at the perimeter is calculated using the linear k-value. The reports resulting from this IEA task (26-31) deal with a wide range of topics concerning fenestration. Information regarding the estimation and use of linear k-values is contained in reference 28. A similar set of linear k-values being considered by the ISO working group on the thermal transmission properties of windows provides more detail in that edge-spacers are categorized as being metal or non-metal (6).

The second procedure (32) for edge-glass U-value calculation is currently being developed as an ASHRAE procedure and is based largely on hot-box results from various laboratories and major manufacturers. This procedure uses prescribed area ratios of frame, edge-glass, and center-glass with the edge-glass U-value being determined as a function of the center-glass U-value. For example, the edge-glass U-value for a standard double-glazed system is 1.2 times greater than the center-glass U-value. In the case of a double-glazed system with a low-e coating the suggested edge/center U-value factor is 1.4. This calculation method is being adapted in order to generate the revised Table 13 of window U-values for the 1989 *ASHRAE Fundamentals*.

The edge-glass calculations outlined above are useful for estimating the thermal losses of windows but they neither provide information about the temperature profiles of individual glazings nor do they fully address the physical mechanisms that determine these temperature profiles. Furthermore, no details are offered regarding the design of the specific edge-seal being considered—even though there are a multitude of designs and sizes on the market. These procedures are of limited utility as aids in the design of more innovative edge-seals.

Two two-dimensional finite-difference computer programs exist that are specifically designed for the analysis of heat loss through window frames. One program was developed in Sweden by Jonsson (33) and the other by Standaert (34) in Belgium. A third program based on the work of Jonsson has been produced by Carpenter (35, 36). A sample of the graphic output taken from the work of Carpenter is shown in Figure 2. These window frame analysis programs calculate a temperature and heat flux solution through the edge-glass area of the glazing system. This is done presumably to set up a more realistic boundary condition for the solution of conductive heat transfer within the frame. Neither the two-dimensional nature of the fill gas flow nor the radiative heat transfer are included in any of these simulation procedures. Heat transfer through the SGU is approximated by treating the sealed cavity as though it were filled with a solid material that is opaque to thermal radiation. This fictitious material is assigned an "effective" thermal conductivity that is determined as a function of the total center-glass heat flux. The absence of fill gas flow is apparent in the symmetry of the isotherms in the fill gas near the end of the glazing cavity. This approach is likely suitable for calculating U-values for frames and the average (top, bottom, and sides) edge-glass heat loss but it is not clear how much accuracy has been forfeited in the edge-glass temperature solution by the extreme simplification of the fill gas/radiation model.

NATURAL CONVECTION BETWEEN GLAZINGS

The two-dimensional analysis of natural convection in the interpane cavity requires treatment of fill gas flow in a tall, vertical, rectangular slot. The fill gas is heated by one of the vertical walls and is cooled by the other. The wall temperatures are not uniform, with the most pronounced variations occurring near the edge-spacers. Similarly, the conditions at the horizontal surfaces are not simple and cannot be specified as having zero heat flux (ZHF) or a linear temperature profile (LTP).

The literature contains an abundance of information about rectangular cavities where a temperature difference between the vertical walls drives a convective flow. It has been shown that the solution is a function of the Rayleigh number, Ra; the aspect ratio of the cavity, A; and the Prandtl number of the fluid, Pr. Relatively few of these papers deal with conditions of interest in the study of convection in glazing units: for air and argon, $Ra < 1.2 \times 10^4$; for gases, $Pr \approx 0.71$ and $A \geqslant 40$. Furthermore, these studies almost universally prescribe isothermal side walls+ and simple boundary conditions, either LTP or ZHF, at the horizontal edges. Nonetheless, it is instructive to review the results of these earlier studies in that useful information is available concerning variables that affect the fill gas flow, the various flow regimes, instabilities in the flow, conditions under which certain flow regimes occur (and can readily be modeled), and details concerning effective modeling. The geometry and some of the nomenclature are shown in Figure 3.

Nusselt first reported heat transfer measurements for this problem in 1909. Since that time many authors have provided additional information (including 18, 37-97). Some studies (18, 37-59) have suggested empirical relationships for the average heat flux over the vertical cavity wall (expressed as a Nusselt number, $Nu = Nu(Ra,Pr,A)$). Most of these correlations cannot be applied to the current problem in that they are not strictly valid for the desired range of Ra (37, 41, 44, 48, 52, 58), Pr (45, 47, 49), or A (37, 41,

\+ Only one study was found (33) where side wall temperatures were not isothermal. Simulation of an SGU was performed with glazing temperature profiles based on hot-box measurements. Computed and measured local heat transfer rates did not agree well.

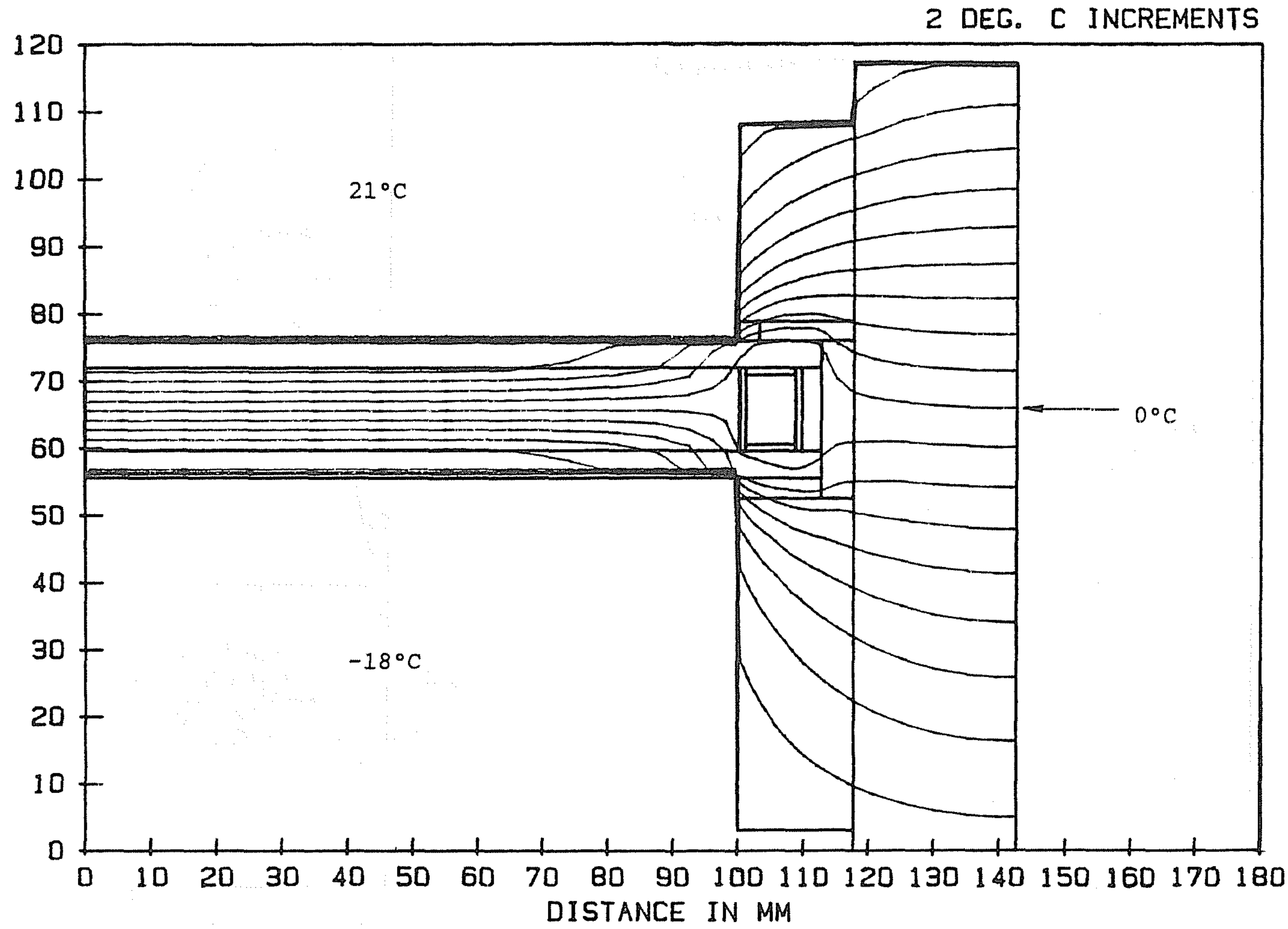

Figure 2 *Plot showing isotherms: standard double-glazed window, wood frame, aluminum spacer (from Carpenter 1987)*

44-47, 49-51, 53, 54, 57-59). Some researchers either neglected or did not discern the dependence of *Nu* on *A* (39, 44, 46, 52, 58). Several correlations remain—the most suitable one being that of ElSherbiny et al. (18) because it was based on a well-established experimental procedure carried out over very wide ranges of *Ra* and *A* with the specific aim of independently resolving the roles of *Ra* and *A*. The *Nu* vs. *Ra* data of ElSherbiny et al. (vertical cavity) are shown in Figure 4. The solid lines plotted in Figure 4 represent the approximate method of Raithby et al. (55).

Batchelor (40) analyzed the laminar natural convection and was the first to define conduction and boundary layer flow regimes. Later, Eckert and Carlson (42) quantified local heat transfer using an interferometer and refined Batchelor's work by proposing conduction, transition, and boundary layer regimes. These flow regimes can be understood by considering the flow at the mid-height of the cavity with *Pr* and *A* held constant. At this location the horizontal velocity component is zero. Figure 5 (based on data from reference 98) shows computed profiles of the vertical velocity component and temperature for three values of *Ra*. When a small temperature difference is applied across the air layer (see $Ra = 10^3$), a weak unicellular flow exists. Air flows up the warm wall, down the cold wall, and the velocity profile on one side of the cavity is influenced by the velocity profile on the opposite side through the shear force between the counterflowing streams. Under this condition the temperature profile across the cavity is linear, heat transfer across the cavity takes place primarily by conduction (except in small regions at the ends of the cavity) with the result that $Nu = 1$. This is called the conduction regime.

When the temperature difference is increased (see $Ra = 10^4$ and 10^5) the flow strengthens and pulls closer to the walls in the form of two increasingly independent boundary layers. Elder (60) and Gill (62) pointed out that the boundary layer thickness is proportional to $Ra^{-1/4}$. At higher values of *Ra* the boundary layers become more distinct and are separated by a core region with the heat transfer taking place more by convection via the boundary layers and less by conduction across the core. In this situation higher horizontal temperature gradients exist at the walls and a smaller horizontal temperature gradient exists in the fluid core. Heat transfer across the cavity is greater than in the conduction regime ($Nu > 1$).

It is noteworthy that no vertical temperature gradient exists in the conduction regime but a vertical temperature gradient does exist within the core once the flow leaves the conduction regime. This temperature gradient is approximately linear with height, except near the ends of the cavity, and creates a stable stratification of the core fluid. The presence of stratification in the core can be used as a

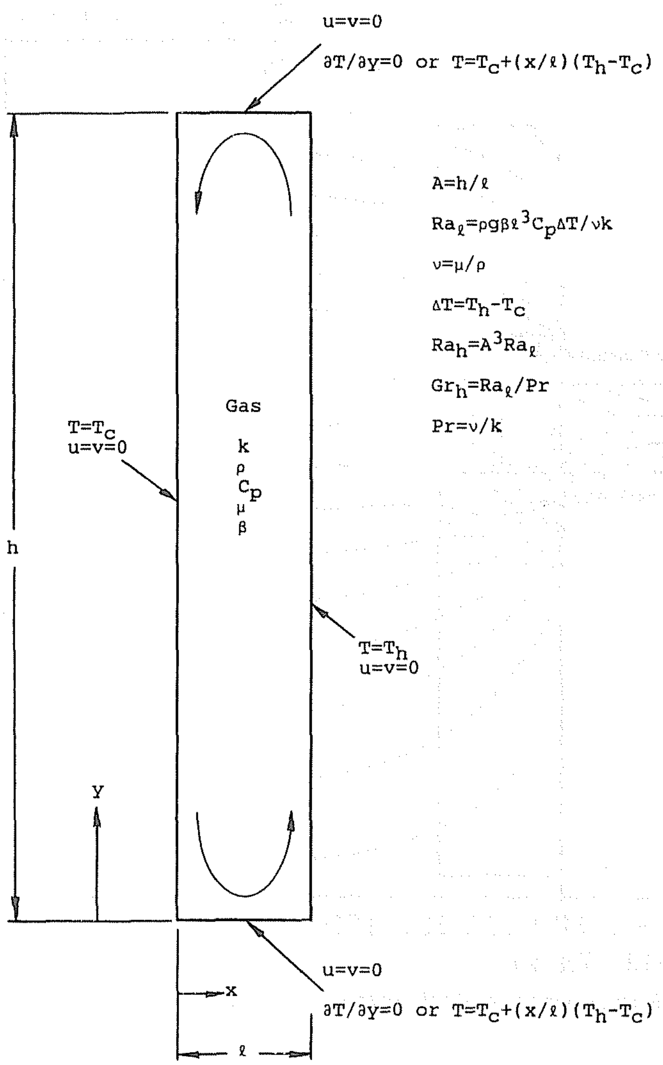

Figure 3 *Problem domain for the analysis of natural convection in a vertical slot*

means of delimiting the conduction regime. More frequently, the nature of the fluid flow is categorized using the non-dimensional horizontal temperature gradient at the mid-point of the cavity, β_h ($\beta_h = -(\partial T/\partial x)(\ell/\Delta T)$, where ΔT is the temperature difference between the vertical walls.

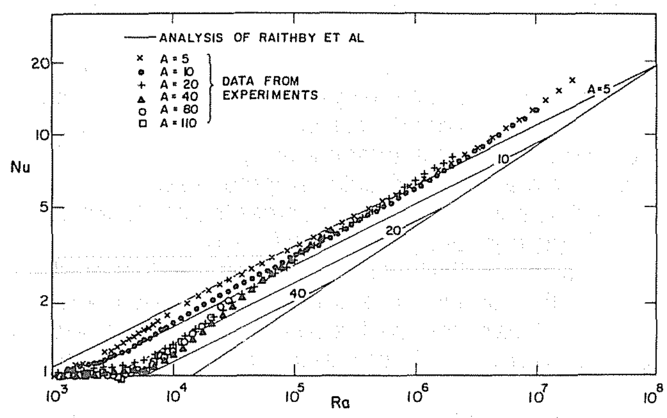

Figure 4 *Nu vs. Ra and A data of ElSherbiny et. al (1982) for air in a vertical cavity*

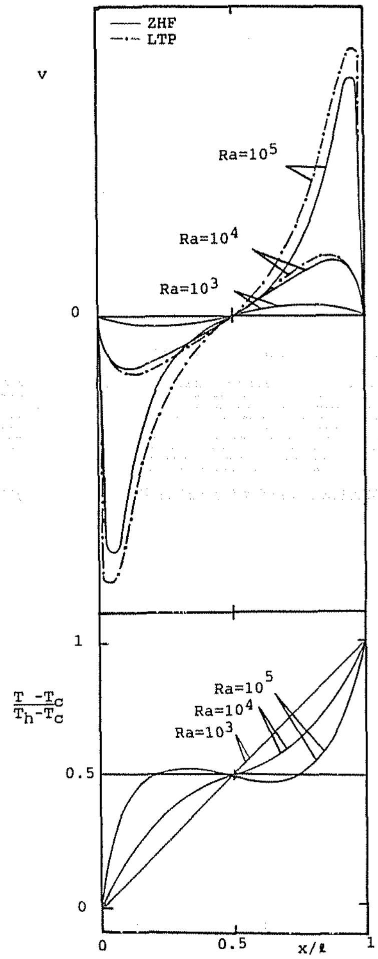

Figure 5 *Computed mid-height velocity and temperature profiles of ElSherbiny et. al (1987), vertical air layer, A = 1*

The conduction regime is characterized by $\beta_h = -1$, the boundary layer regime by $\beta_h \geqslant 0$, and the transition regime by $-1 < \beta_h < 0$. The three curves shown in the lower portion of Figure 5 are typical of temperature profiles for each of these three laminar flow regimes. A good discussion regarding the balance between shear and buoyant forces occurring in the conduction and boundary layer regimes is given by Raithby et al. (55).

The critical value of *Ra* at which flow leaves the conduction regime lies in the range $10^3 < Ra < 6 \times 10^3$ and is a function of *A*. This aspect ratio dependence can be seen in Figure 4. The convective flow leaves the conduction regime at lower values of *Ra* in cavities with lower *A* values.

If *Ra* is increased sufficiently, instabilities occur that create time-dependent flow and eventually a turbulent boundary layer flow. The transition from laminar to turbulent flow can readily be pinpointed in the approximate method of Raithby et al. shown in Figure 4. The turbulent flow condition is represented by the line that extends upward to the right with a slope of 1/3. The lines inside the knee created by the turbulent boundary layer line and the horizontal axis have a slope of 1/4 and represent laminar boundary layer flow for various values of *A*. The critical value of *Ra* for the onset of turbulent flow is a function of *A*. The flow in enclosures with larger aspect ratios becomes

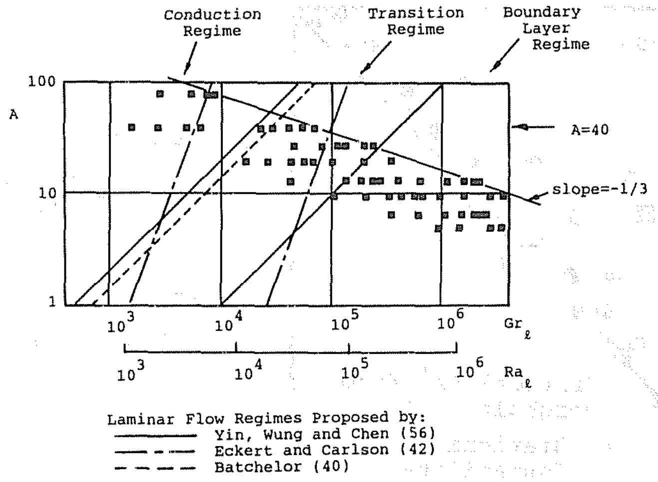

Figure 6 *Laminar flow regimes (from Yin et. al 1978)*

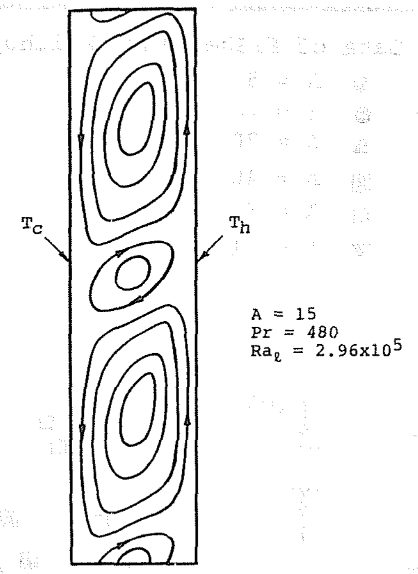

Figure 7 *Sketch of secondary and tertiary flow (based on Seki et. al 1978)*

turbulent at smaller values of *Ra*. The results of this theory suggest that the flow in very tall, narrow slots can become turbulent directly from the conduction regime without passing through the laminar transition or laminar boundary layer regimes.

The experimental data shown in Figure 4 display some trends that are similar to those of the theory. However, they do not show the ordered progression (as a function of *A*) that might be expected inside the knee. The measured *Nu* vs. *Ra* curves are tightly grouped and for $A > 20$ they all depart the conduction regime at $Ra \approx 6 \times 10^3$. It is tempting to conclude, on the basis of the general similarity between the shapes of the measured and theoretical curves, that the flow immediately enters the turbulent regime. However, it is not clear whether *Nu* increases because the flow enters the laminar boundary layer regime, because it becomes turbulent, or because of some other phenomenon.

A clue regarding the nature of the flow at $Ra > 6 \times 10^3$ can be taken from the work of Yin et al. (56), who made heat transfer and temperature profile measurements on air-filled cavities of high aspect ratio and with $1.1 \times 10^3 < Ra < 5 \times 10^6$. In Figure 6 data taken from reference 56 are reproduced. Values of *Gr* and *A* for which Yin et al. reported their measurements are shown and ranges of *Ra* and *A* over which they (and others) felt the conduction, transition, and boundary layer regimes occur are presented. Elder (61) proposed lines that mark the onset of "wavelike" motions ($Ra > 8 \times 10^8 Pr^{0.5} A^{-3}$) and turbulence ($Ra > 10^{10} A^{-3}$) based on his experiments using water ($Pr \approx 7$). The slope of these lines corresponds well to the upper limit for which Yin et al. reported experimental data. (A line of slope = $-1/3$ has been superimposed on Figure 6.) Yin et al. stated that temperature fluctuations occurred for high *Ra* and that data were reported only for experiments in which no fluctuations were measured. This statement suggests that a steady, laminar flow existed over the ranges of *Ra* and *A* for which data were reported. At $A = 40$, for example, a steady, laminar flow persists for *Ra* well in excess of 10^4. The data shown in Figure 7 also support the idea that turbulence commences at lower values of *Ra* for cavities with larger aspect ratios—keeping in mind that the data shown in Figure 4 show that turbulence does not occur below $Ra \approx 6 \times 10^3$ even for very large aspect ratios.

The analysis of the laminar natural convection in a vertical slot requires more than the simple consideration of conduction, transition, and boundary layer flows. In 1965 Elder (60) reported on visualization experiments, using paraffin and silicone oil, in which he detected a steady secondary flow. This secondary flow consisted of a regular "cats-eye" pattern of cells within the core of the base flow—with the flow in each cell rotating in the same direction as the base flow. At certain values of *Ra* counter-rotating cells (tertiary cells) were found in the regions between the secondary cells. Cellular patterns have also been visualized by Vest and Arpaci (64) in air, Korpela (72) in air, Seki et al. (79) in transformer oil and glycerin, and Choi and Korpela (82) in air. Figure 7 shows a sketch of secondary and tertiary cells shown in reference 79.

The nature of flow in the conduction and boundary layer regimes has been studied (63-68, 70-72, 76, 77, 79, 82) and attempts to predict the critical Rayleigh number, Ra_c, at which hydrodynamic instability causes the onset of secondary flow have been made. These predictions (for $Pr \approx 0.71$) fall in a relatively narrow band, ranging from Ra_c =5595 (Vest and Arpaci [64]) to Ra_c = 7827 (Unny [68]). Vest and Arpaci (64) made a visual measurement of Ra_c = 6177 ±10%. Hollands and Konicek (70) used a calorimetric method to determine Ra_c = 7810 ±362.

The physical balances governing the behavior of the fill gas can be represented by mathematical expressions for the conservation of mass, momentum, and energy. Simplified expressions describing the laminar 2-D fill-gas flow can be written by assuming that the fluid is Newtonian, compressibility effects and viscous dissipation can be neglected, and that fluid properties can be taken as constant except in the formulation of the buoyancy term. Leonardi and Reizes (93) examined the assumption of constant fluid properties and demonstrated its validity for cases

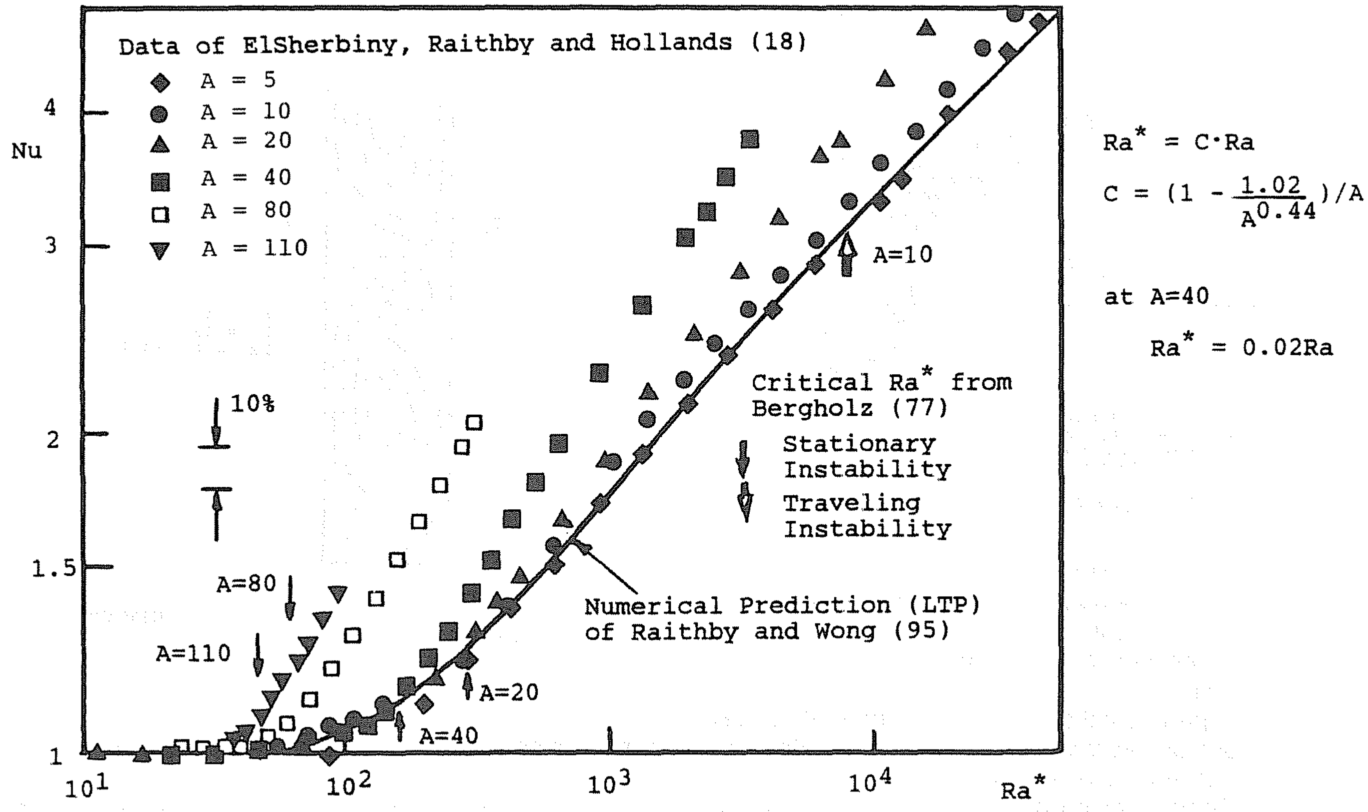

Figure 8 *Comparison of predictions of Raithby and Wong (1981) (solid curve) with experimental data (ElSherbiny et. al 1982)*

where the temperature variation is less than 10% of the mean (absolute) temperature.

A variety of authors (including 41, 47-51, 73, 86-91, 93-97) present numerical solutions to the equations of motion for a fluid in a rectangular enclosure with differentially heated vertical walls and either ZHF or LTP horizontal boundary conditions. The large majority of these studies do not address the problem of high aspect ratio. However, Raithby and Wong (94) provide finite-difference predictions for heat transfer across vertical air layers with $2 < A < 80$ and $10^3 < Ra < 3 \times 10^5$. A comparison between their results and the experimental results of ElSherbiny et al. (18) is shown in Figure 8 (data taken from ref. 94). Raithby and Wong (94) were able to collapse the results of all aspect ratios onto a single curve (solid line in Figure 8) by plotting Nu vs. Ra^*. Ra^* is obtained by multiplying Ra by a factor that was a function of A only. Raithby and Wong have also calculated the values of Ra^* at which hydrodynamic instabilities are expected to occur. These calculations were performed using the method of Bergholz (77). Figure 8 shows that, for each set of experimental data at a specific value of A, the predicted rate of heat transfer closely corresponds to the measured rate of heat transfer up to the critical value of Ra (or Ra^*) at which hydrodynamic instability is predicted and at which the onset of secondary flow is expected. This difference between the measured and predicted results can readily be explained because secondary cells were not predicted by the analysis of Raithby and Wong. Raithby and Wong suggested that the secondary and tertiary flows might have been resolved if a finer grid had been used.

Subsequently, Lee and Korpela (95) numerically modeled laminar air flow in a vertical slot for $3.5 \times 10^3 < Ra < 1.75 \times 10^5$. The results of this simulation included the onset of secondary cells at Ra_c between 7×10^3 and 7.7×10^3 with $A = 20$. Streamline results for various values of Ra are shown in Figure 9. Lee and Korpela also compared their predicted values of Nu with the experimental results of ElSherbiny et al. This comparison is shown in Figure 10 (data taken from reference 95). In this case, the predicted heat transfer rates were in close agreement with the measured heat transfer rates to appreciably higher values of Ra than was the case with the predictions of Raithby and Wong. For instance, at $A = 40$ and $Ra = 2 \times 10^4$, the predictions of Lee and Korpela agree with experiments to within 10% while the predictions of Raithby and Wong show a discrepancy of 10% by $Ra^* \approx 247$ ($Ra \approx 1.2 \times 10^4$). The improved agreement with measurement was attributed directly to their ability to resolve the secondary cells. However, the results of Lee and Korpela consistently underpredict the measured values of Nu at higher values of Ra ($Ra > 1.2 \times 10^4$ for $A = 40$). This may be a result of the failure of their method to resolve a tertiary fluid flow. Alternatively, it is possible that $Ra = 1.2 \times 10^4$ marks the onset of turbulence.

More recently, Korpela et al. (98) showed that the results of Bergholz (77) could be simplified to predict the critical value of Gr, based on the cavity height, h, at which the onset of secondary cells takes place from the conduction regime. This was expressed as:

$$Gr_h = (A^3 + 5A^2)/1.25 \times 10^{-4} \qquad [1]$$

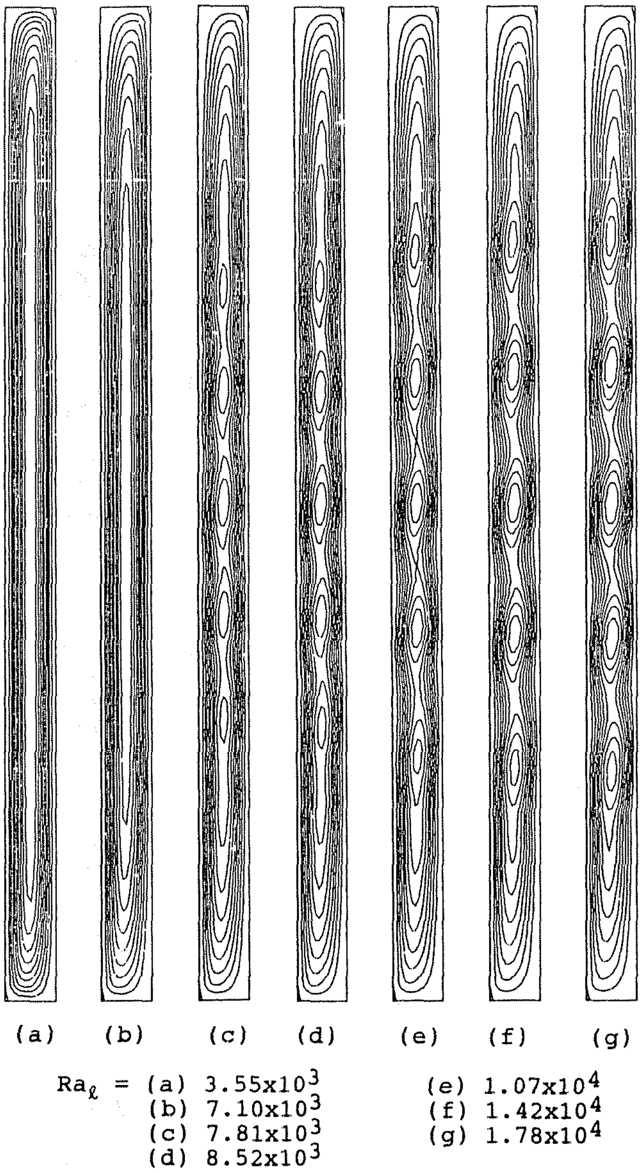

Figure 9 *Numerical streamline solutions of Lee and Korpela (1983) with experimental data (ElSherbiny et. al 1982)*

This expression can be converted to predict the critical Grashof number based on ℓ instead. In this case,

$$Gr_\ell = (1 + 5/A)/1.25 \times 10^{-4} \quad [2]$$

In a window cavity, where A is typically very large, Equation 2 predicts the onset of secondary cells at $Gr_\ell = 8 \times 10^3$ or $Ra_\ell \approx 5.6 \times 10^3$.

Many experimental and numerical studies provide information regarding the local rate of convective heat transfer. Data taken from the numerical solution of Korpela et al. (98) are plotted in Figure 11. Figure 11 shows the local Nusselt number (denoted $Nu_\ell(y)$) as a function of the distance from the bottom of the cavity, y. $Nu_\ell(y)$ is based on the heat flux at the warm vertical wall. The three curves shown correspond to three values of Ra. When Ra is sufficiently small (see $Ra = 3550$) the flow is in the conduction regime and $Nu_\ell(y) = 1$, except at the ends of the cavity. At higher values of Ra the rate of heat transfer increases in most regions and the wave-like nature of the curves in the

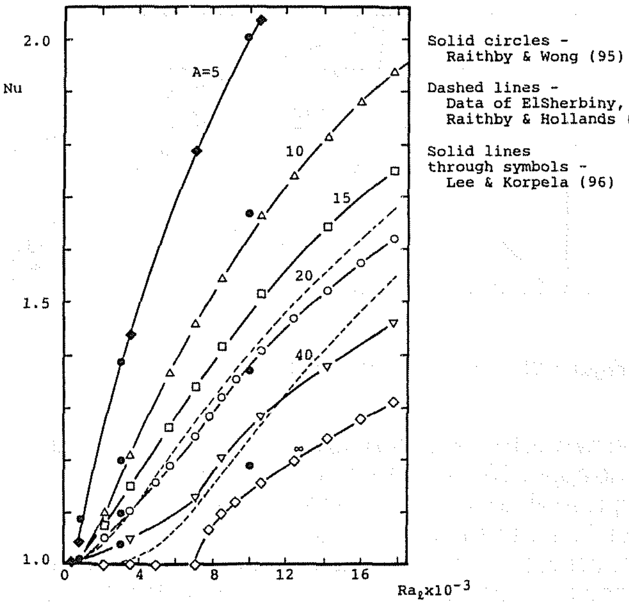

Figure 10 *Comparison of predictions of Lee and Korpela (1983) with experimental data (ElSherbiny et. al 1982)*

middle portion of the cavity indicates that secondary cells are present.

DISCUSSION

A simplified version of Figure 6 is given in Figure 12. The lines suggested by Yin et al. (56) to delimit the laminar flow regimes are shown along with the line of slope = −1/3

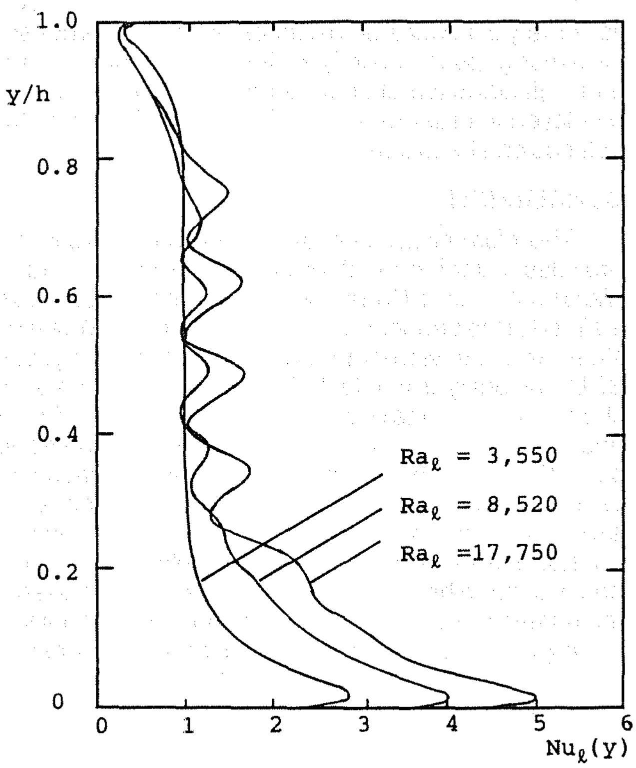

Figure 11 *Local Nusselt number, Nu (y) for A = 20 based on data from Korpela et. al (1982)*

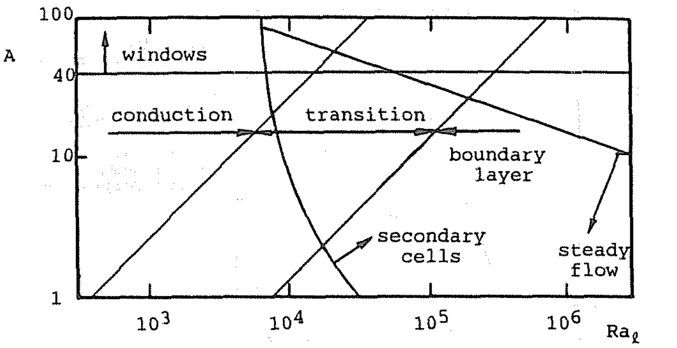

Figure 12 *Convective flow regimes for vertical window cavities*

below which steady flow is expected. The region of aspect ratio applicable to windows ($A > 40$) is marked and the line representing the onset of secondary cells, given by Equation 2, is also shown. It can be seen that the character of the convective flow in a window cavity is likely to move from conduction directly into secondary or turbulent flow as Ra increases. It is unlikely that either laminar transition or laminar boundary flows will exist.

Under the ASHRAE winter design condition, calculations (using VISION) show that $Ra_\ell \approx 6.6 \times 10^3$ ($Gr_\ell \approx 9.3 \times 10^3$) for a conventional double glazed window (½ in pane spacing) and $Ra_\ell \approx 8.3 \times 10^3$ ($Gr_\ell \approx 1.2 \times 10^4$) for the same window with a soft low-e coating. Corresponding values of Ra_ℓ for similar windows with argon fill gas are about 25% higher. If krypton is used in place of air with the same pane spacing, then Ra_ℓ will be higher by a factor of about 4.5. When air or argon fill gas is used with ½ in edge-seals then the motion of the fill gas will be laminar and free of secondary cells under most conditions with the exception of very cold weather. In contrast, when krypton is used narrower gaps (smaller ℓ) and/or glazing systems with more glazings (smaller ΔT across each gap) must be employed in order to reduce Ra to the point where turbulence can be avoided.

CONCLUSION

The information summarized in the previous sections provides a starting point for detailed research in edge-glass heat transfer. Current work at a Canadian university is aimed at the development of a finite-volume (99), steady-state, two-dimensional model of a vertical, double-glazed SGU. The analysis will deal with natural convection of the fill gas, the exchange of thermal radiation, and conductive heat transfer along the glazings and through the edge-seals. Boundary conditions applied initially will correspond to the conditions imposed on a sealed glazing unit during experimental testing in a guarded heater plate apparatus (2). This enables a direct comparison between computed and measured heat flux results. Following this initial test of the numerical model more realistic boundary conditions corresponding to the indoor/outdoor environment can be incorporated in order to estimate temperature profiles along the individual glazings.

REFERENCES

1. Solvason, K.R. 1974. "Pressures and stresses in sealed double glazing units." National Research Council of Canada, Division of Building Research, Technical Paper No. 423.
2. Wright, J.L., and Sullivan, H.F. 1988. "Glazing system U-value measurement using a guarded heater plate apparatus." *ASHRAE Transactions,* Vol. 94, Part 2, pp. 1325-1337.
3. Parmalee, G.V. 1947. "Heat transmission through glass." *ASHVE Research Bulletin,* Vol. 53, No. 1.
4. McCabe, M.E., and Goss, W.P. 1987. "Interim procedure to measure the thermal performance of window systems." Prepared by the National Bureau of Standards, Report No. NBSIR 87)3569, for the Bonneville Power Administration.
5. ISO. 1986. Proposed ISO Standard, "Thermal insulation of glazing: calculation rules for determining the steady state 'U' value (thermal transmittance) of double or multiple glazing." ISO TC 160, SC2, Working Group 2, 4th revision.
6. Curcija, D.; Ambs, L.L.; and Goss, W.P. 1989. "A comparison of European and North American window U-value calculation procedures." *ASHRAE Transactions,* Vol. 95, Part 1.
7. Ferguson, J.E., and Wright, J.L. 1984. "A computer program to evaluate the thermal performance of super windows." National Research Council of Canada, Division of Energy Report No. Passive-10, June.
8. Wright, J.L., and Sullivan, H.F. 1987a. "VISION: A computer program for the detailed simulation of the thermal performance of innovative glazing systems." International Conference on Building Energy Management, Lausanne, Switzerland.
9. Wright, J.L., and Sullivan, H.F. 1987b. "VISION: A computer program to evaluate the thermal performance of innovative glazing systems—reference manual." Report produced by the Advanced Glazing Systems Laboratory, Department of Mechanical Engineering, University of Waterloo, Waterloo, Canada.
10. Sullivan, H.F., and Wright, J.L. 1987. "Recent improvements and sensitivity of the VISION glazing system thermal analysis program." *Proceedings of the 12th Passive Solar Conference,* ASES/SESCI, Portland, OR, pp. 145-149.
11. Baker, J.A.; Sullivan, H.F.; and Wright, J.L. 1988. "Screen graphics software for the VISION glazing system analysis program." Proceedings of the Solar Energy Society of Canada Inc., Ottawa.
12. Wright, J.L. 1980. "Free convection in inclined air layers constrained by a V-corrugated teflon film." M.A.Sc. thesis, Department of Mechanical Engineering, University of Waterloo, Waterloo, Canada.
13. Hollands, K.G.T., and Wright, J.L. 1980. "Theory and experiment on heat loss coefficients for plastic covers." *Proceedings of the American Section of the International Solar Energy Society,* pp. 441-445. Phoenix.
14. Hollands, K.G.T., and Wright, J.L. 1982. "Heat loss coefficients and effective $\tau\alpha$ products for flat-plate collectors with diathermanous covers." *Solar Energy,* Vol. 30, pp. 211-216.
15. Harrison, S.J., and Barakat, S.A. 1983. "A method for comparing the thermal performance of windows." *ASHRAE Transactions,* Vol. 89, Part 1, pp. 3-11.
16. Barakat, S.A. 1985. "Comparison of the thermal performance of glazing systems." Proceedings of the ISES/SESCI Intersol '85 Conference, Montreal, Canada.
17. Ferguson, J.E., and Wright, J.L. 1985. "Optimization of glazing design for residential use." Proceedings of the ASHRAE/DOE/BTECC Thermal Performance of the Exterior Envelope of Buildings Conference, Clearwater, FL, December.
18. ElSherbiny, S.M.; Hollands, K.G.T.; and Raithby, G.D. 1982. "Effect of thermal boundary conditions on natural convection in vertical and inclined air layers." *Journal of Heat Transfer,* Vol. 104, pp. 515-520.
19. Rubin, M. 1982. "Calculating heat transfer through windows." *International Journal of Energy Research,* Vol. 6, No. 4.
20. Bowen, R.P. 1985. "DBR's approach for determining the heat transmission characteristics of windows." NRC Building Research Note BRN 234.

21. McCabe, M.E., and Hill, D. 1987. "Field measurement of thermal and solar/optical properties of insulating glass windows." *ASHRAE Transactions*, Vol. 93, Part 1, pp. 1409-1424.
22. Klems, J.H., and Keller, H. 1987. "Measurement of fenestration thermal performance under realistic conditions using the mobile window thermal test (MoWiTT) facility." International Conference on Building Energy Management, Lausanne, Switzerland.
23. Eggimann, J.P., and Faist, A. 1987. "The double-skin wall: a promising solar facade." International Conference on Building Energy Management, Lausanne, Switzerland, September.
24. Barakat, S.A. 1984. "NRCC passive solar test facility description and data reduction." DBR/NRC Technical Note BRN 214.
25. Frank, T., and Muehlebach, H. 1987. "Coefficient de transmission thermique des fenetres." Taken from an article in *Ingnieurs et architectes Suisses*.
26. IEA. 1986a. Windows and fenestration, step 1—building regulations, standards and codes concerning thermal and solar performance of windows; a survey of eight countries. Energy Conservation in Buildings and Community Systems Programme, Annex XII.
27. IEA. 1986b. Windows and fenestration, step 2—thermal transmission through windows (selected examples to illustrate the need for a more standardized approach). Energy Conservation in Buildings and Community Systems Programme, Annex XII.
28. IEA. 1986c. Windows and fenestration, step 2—thermal and solar properties of windows (expert guide).
29. IEA. 1986d. Windows and fenestration, step 3—calculation of seasonal heat loss and gain through windows; a comparison of some simplified models. Energy Conservation in Buildings and Community Systems Programme, Annex XII.
30. IEA. 1986e. Windows and fenestration, step 4—comparison of six simulation codes DEROB, DYWON, PASSIM, DOE-2.1C, SERI—RES, HELIOS1. Energy Conservation in Buildings and Community Systems Programme, Annex XII.
31. IEA. 1986f. Windows and fenestration, step 5—windows and space heating requirements (parameter studies leading to a simplified calculation method). Energy Conservation in Buildings and Community Systems Programme, Annex XII.
32. Peterson, C.O. 1987. "How is low-E performance criteria determined?" *Glass Digest*.
33. Jonsson, B. 1985. "Heat transfer through windows during the hours of darkness with the effect of infiltration ignored." Swedish Council for Building Research Report, Document D13:1985.
34. KOBRU86. 1986. "Computer program to calculate two dimensional steady state heat transfer in objects, described in a rectangular grid, using the energy balance technique. Alphanumerical input, alphanumerical and graphical output." Information brochure.
35. Carpenter, S.C. 1987. "The effect of frame design on window heat loss—phase 1." Report prepared by Enermodal Engineering Ltd. for Energy, Mines and Resources Canada.
36. Carpenter, S.C., and McGowan, A. 1988. "Calculating window U-values including frame effects" Proceedings of the 14th Annual Conference of the Solar Energy Society of Canada Inc., Ottawa.
37. Jakob, M. 1946. "Free heat convection through enclosed plane gas layers." *Trans. Amer. Soc. Mech. Eng.*, Vol. 68, pp. 189-194.
38. Peck, R.E.; Fagan, W.S.; and Werlein, P.P. 1951. "Heat transfer through gases at low pressures." *Trans. ASME*, Vol. 73, pp. 281-287.
39. DeGraaf, J.G.A., and Van Der Held, E.F.M. 1953. "The relation between the heat transfer and convection phenomena in enclosed plane air layers." *Applied Science Research*, Vol. 3, pp. 393-409.
40. Batchelor, G.K. 1954. "Heat transfer by free convection across a closed cavity between vertical boundaries at different temperatures." *Quarterly of Applied Mathematics*, Vol. 12, pp. 209-233.
41. Poots, G. 1958. "Heat transfer by laminar free convection in enclosed plane gas layers." *Quart. J. Mech. Appl. Math.*, Vol. 11, pp. 257-267.
42. Eckert, E.R.G., and Carlson, W.O. 1961. "Natural convection in an air layer enclosed between two vertical plates with different temperatures." *International Journal of Heat and Mass Transfer*, Vol. 2, pp. 106-120.
43. Emery, A.F. 1963. "The effect of a magnetic field upon the free convection of a conducting fluid." *Journal of Heat Transfer*, Series C, Vol. 85, pp. 119-124.
44. Dropkin, D., and Somerscales, E. 1965. "Heat transfer by natural convection in liquids confined by two parallel plates which are inclined at various angles with respect to the horizontal." *Journal of Heat Transfer*, Series C, Vol. 87, pp. 77-84.
45. Emery, A.F., and Chu, N.C. 1965. "Heat transfer across vertical layers." *Journal of Heat Transfer*, Series C, Vol. 87, pp. 110-116.
46. Landis, F., and Yanowitz, H. 1966. "Transient natural convection in a narrow vertical cell." *Transactions, International Heat Transfer Conference*, pp. 139-151.
47. Elder, J.W. 1966. "Numerical experiments with free convection in a vertical slot." *J. Fluid Mechanics*, Vol. 24, p. 823.
48. de Vahl Davis, G. 1968. "Laminar natural convection in an enclosed rectangular cavity." *International Journal of Heat and Mass Transfer*, Vol. 11, pp. 1675-1693.
49. MacGregor, R.K., and Emery, A.F. 1969. "Free convection through vertical plane layers—moderate and high Prandtl number fluids." *Journal of Heat Transfer*, pp. 391-403.
50. Newell, M.E., and Schmidt, F.W. 1970. "Heat transfer by laminar natural convection within rectangular enclosures." *Journal of Heat Transfer*, Series C, Vol. 92, pp. 159-165.
51. Thomas, R.W. 1970. "Natural convection in annular and rectangular cavities—a numerical study." Proceedings of the International Heat Transfer Conference, Paris.
52. Jannot, M., and Mazeas, C. 1973. "Etude experimentale de la convection naturelle dans des cellules rectangulaires, verticales." *International Journal of Heat and Mass Transfer*, Vol. 16, pp. 81-100.
53. Mynett, J.A., and Duxbury, D. 1974. "Temperature distributions within enclosed plane air cells associated with heat transfer by natural convection." *Proceedings of the 1974 International Heat Transfer Conference*, pp. 119-123. Tokyo.
54. Berkovsky, B.M., and Polevikov, V.K. 1977. "Numerical study of problems on high-intensive free convection." *Heat Transfer and Turbulent Buoyant Convection*, Vols. 1 and 2, pp. 443-455. Eds. Spalding and Afgan. Hemisphere Publishing Corp.
55. Raithby, G.D.; Hollands, K.G.T.; and Unny, T. 1977. "Analysis of heat transfer by natural convection across vertical fluid layers." *Journal of Heat Transfer*, Vol. 99, pp. 287-293.
56. Yin, S.H.; Wung, T.Y.; and Chen, K. 1978. "Natural convection in an air layer enclosed within rectangular cavities." *International Journal of Heat and Mass Transfer*, Vol. 21, pp. 307-315.
57. Seki, N.; Fukusako, S.; and Inaba, H. 1978b. "Heat transfer of natural convection in a rectangular cavity with vertical walls of different temperatures." *Bulletin of the JSME*, Vol. 21, No. 152.
58. Schinkel, W.M.M., and Hoogendoorn, C.J. 1978. "An interferometric study of the local heat transfer by natural convection in inclined air-filled enclosures." *Proceedings of the 1978 International Heat Transfer Conference* (Toronto), pp. 287-292.
59. Randall, K.R.; Mitchell, J.W.; and El-Wakil, M.M. 1979. "Natural convection heat transfer characteristics of flat plate enclosures." *Journal of Heat Transfer*, Vol. 101, pp. 120-125.
60. Elder, J.W. 1965a. "Turbulent free convection in a vertical slot." *Journal of Fluid Mechanics*, Vol. 23, Part 1, pp. 77-98.

61. Elder, J.W. 1965b. "Laminar free convection in a vertical slot." *Journal of Fluid Mechanics,* Vol. 23, Part 1, pp. 99-111.
62. Gill, A.E. 1966. "The boundary-layer regime for convection in a rectangular cavity." *Journal of Fluid Mechanics,* Vol. 26, Part 3, pp. 515-536.
63. Birikh, R.V.; Gershuni, G.Z.; Zhukhovitskii, E.M.; and Rudadov, R.N. 1968. "Hydrodynamic and thermal instability of a steady convection flow." *Prikl. Mat. Mekh.,* Vol. 32, No. 2, pp. 256-263.
64. Vest, C.M., and Arpaci, V.S. 1969. "Stability of natural convection in a vertical slot." *Journal of Fluid Mechanics,* Vol. 36, Part 1, pp. 1-15.
65. Gill, A.E., and Davey, A. 1969. "Instabilities of a buoyancy-driven system." *Journal of Fluid Mechanics,* Vol. 35, Part 4, pp. 775-798.
66. Gill, A.E., and Kirkham, C.C. 1970. "A note on the stability of convection in a rectangular slot." *Journal of Fluid Mechanics,* Vol. 42, Part 1, pp. 125-127.
67. Hart, J.E. 1971. "Stability of the flow in a differentially heated inclined box." *Journal of Fluid Mechanics,* Vol. 47, Part 3, pp. 547-576.
68. Unny, T.E. "Thermal instability in differentially heated inclined fluid layers." *Journal of Applied Mathematics,* pp. 41-46.
69. Brooks, R.G., and Probert, S.D. 1972. "Heat transfer between parallel walls: an interferometric investigation." *Journal of Mechanical Engineering Science,* Vol. 14, No. 2, pp. 107-127.
70. Hollands, K.G.T., and Konicek, L. 1973. "Experimental study of the stability of differentially heated inclined air layers." *International Journal of Heat and Mass Transfer,* Vol. 16, pp. 1467-1476.
71. Korpela, S.A.; Gozum, D.; and Baxi, C. 1973. "On the stability of the conduction regime of natural convection in a vertical slot." *International Journal of Heat and Mass Transfer,* Vol. 16, pp. 1683-1690.
72. Korpela, S.A. 1974. "A study on the effect of Prandtl number on the stability of the conduction regime of natural convection in an inclined slot." *International Journal of Heat and Mass Transfer,* Vol. 17, pp. 215-222.
73. Catton, E.; Ayyaswamy, P.S.; and Clever, R.M. 1974. "Natural convection flow in a finite, rectangular slot arbitrarily oriented with respect to the gravity vector." *International Journal of Heat and Mass Transfer,* Vol. 17, pp. 473-484.
74. Dixon, M., and Probert, S.D. 1975. "Heat-transfer regimes in vertical, plane-walled, air-filled cavities." *International Journal of Heat and Mass Transfer,* Vol. 18, pp. 709-710.
75. Dulnev, G.N.; Zarichnyak, Y.P.; and Sharkov, A.V. 1975. "Free convection at a vertical plate and in closed interlayer at different gas pressures." *International Journal of Heat and Mass Transfer,* Vol. 18, pp. 213-218.
76. Clever, R.M., and Busse, F.H. 1977. "Instabilities of longitudinal convection rolls in an inclined layer." *Journal of Fluid Mechanics,* Vol. 81, Part 1, pp. 107-127.
77. Bergholtz, R.F. 1978. "Instability of steady natural convection in a vertical fluid layer." *Journal of Fluid Mechanics,* Vol. 84, Part 4, pp. 743-768.
78. Morrison, G.L., and Tran, V.Q. 1978. "Laminar flow structure in vertical free convective cavities." *International Journal of Heat and Mass Transfer,* Vol. 21, pp. 203-213.
79. Seki, N.; Fukusako, S.; and Inaba, H. 1978a. "Visual observation of natural convective flow in a narrow vertical cavity." *Journal of Fluid Mechanics,* Vol. 84, Part 4, pp. 695-704.
80. Catton, I. 1978. "Natural convection in enclosures." Proceedings of the International Heat Transfer Conference, Toronto, Canada.
81. Bejan, A. 1979. "Note on Gill's solution for free convection in a vertical enclosure." *Journal of Fluid Mechanics,* Vol. 90, Part 3, pp. 561-568.
82. Choi, I.G., and Korpela, S.A. 1980. "Stability of the conduction regime of natural convection in a tall vertical annulus." *Journal of Fluid Mechanics,* Vol. 99, Part 4, pp. 725-738.
83. Graebel, W.P. 1981. "The influence of Prandtl number on free convection in a rectangular cavity." *International Journal of Heat and Mass Transfer,* Vol. 24, pp. 125-131.
84. ElSherbiny, S.M.; Raithby, G.D.; and Hollands, K.G.T. 1982. "Heat transfer by natural convection across vertical and inclined air layers." *Journal of Heat Transfer,* Vol. 104.
85. ElSherbiny, S.M.; Hollands, K.G.T.; and Raithby, G.D. 1983. "Nusselt number distribution in vertical and inclined air layers." *Transactions of the ASME,* Vol. 105, pp. 406-408.
86. Quon, C. 1972. "High Rayleigh number convection in an enclosure—a numerical study." *The Physics of Fluids,* Vol. 15, No. 1, pp. 12-19.
87. Mallinson, G.D., and de Vahl Davis, G. 1973. "The method of the false transient for the solution of coupled elliptic equations." *Journal of Computational Physics,* Vol. 12, pp. 435-461.
88. Spradley, L.W., and Churchill, S.W. 1975. "Pressure and buoyancy-driven thermal convection in a rectangular enclosure." *Journal of Fluid Mechanics,* Vol. 70, Part 4, pp. 705-720.
89. de Vahl Davis, G., and Mallinson, G.D. 1975. "A note on natural convection in a vertical slot." *Journal of Fluid Mechanics,* Vol. 72, Part 1, pp. 87-93.
90. Mallinson, G.D., and de Vahl Davis, G. 1977. "Three-dimensional natural convection in a box: a numerical study." *Journal of Fluid Mechanics,* Vol. 83, Part 1, pp. 1-31.
91. Wong, H.H., and Raithby, G.D. 1979. "Improved finite-difference methods based on a critical evaluation of the approximation errors." *Numerical Heat Transfer,* Vol. 2, pp. 139-163.
92. Jones, I.P. 1979. "A comparison problem for numerical methods in fluid dynamics, the 'double-glazing' problem." *Proceedings of the International Heat Transfer Conference,* pp. 338-348.
93. Leonardi, E., and Reizes, J.A. 1979. "Natural convection in compressible fluids with variable properties." *Proceedings of the International Heat Transfer Conference,* pp. 297-306.
94. Raithby, G.D., and Wong, H.H. 1981. "Heat transfer by natural convection across vertical air layers." *Numerical Heat Transfer,* Vol. 4, pp. 447-457.
95. Lee, Y., and Korpela, S.A. 1983. "Multicellular natural convection in a vertical slot." *Journal of Fluid Mechanics,* Vol. 126, pp. 91-121.
96. de Vahl Davis, G. 1983. "Natural convection of air in a square cavity: a benchmark numerical solution." *International Journal for Numerical Methods in Fluids,* Vol. 3, pp. 249-264.
97. ElSherbiny, S.M.; Fath, H.E.S.; and Refai, G.A. 1987. "Numerical analysis of natural convection in vertical and inclined air layers." Submitted for publication in *Journal of Heat and Fluid Flow.*
98. Korpela, S.A.; Lee, Y.; and Drummond, J.E. 1982. "Heat transfer through a double pane window." *Journal of Heat Transfer,* Vol. 104, pp. 539-544.
99. Patankar, S.V. 1980. *Numerical heat transfer and fluid flow.* Hemisphere Publishing Corp.

DISCUSSION

T.F. Smith, Professor, Univ. of Iowa Dept. of Mechanical Engineering, Iowa City: It should be realized that for most window heat transfer applications the Rayleigh number is around 10^4. Hence, this places the analysis in the conduction regime shown in Figure 12.

J.L. Wright: The problem of interest, namely the occurrence of condensation on the indoor glazing, requires the study of relatively severe weather conditions rather than a more moderate condition that is representative of what the window is exposed to over a long time or on average. The discussion section of the paper lists

Rayleigh numbers that might be expected in several common glazing unit designs for the ASHRAE winter design condition. They are all near 10^4 but all are greater than the critical value of Rayleigh (5600) and instead of operating in the conduction regime, secondary cells, or perhaps turbulence, can be expected depending on the aspect ratio of the cavity.